Optical/digital color photography based on white-light information processing

LUO Gang (罗 罡)[1], LIU Fulai (刘福来)[1], LIN Lie (林 列)[1], FANG Zhiliang (方志良)[1], WANG Zhaoqi (王肇圻)[1], WEN Zhicheng (翁志成)[2] & MU Guoguang (母国光)[1]

1. Institute of Modern Optics, Nankai University, Tianjin 300071; Tianjin United Scientific Research Center on Opto-electronics, Tianjin 300071, China;
2. Changchun Institute of Optical and Fine Mechanics, Chinese Academy of Sciences, Changchun 130022, China

Correspondence should be addressed to Luo Gang.

Received May 25, 2000

Abstract The achievement in optical/digital color photography based on white-light information processing including the color-encoding camera, the color image decoder, the integral window Fourier algorithm of the Fourier transform in digital decoding, the color correction of the retrieval color image and the fusion of zero order diffraction is reported. This technique has found its important applications in the fields of aerial reconnaissance photography and far-distance ground photography due to its features of large information capacity, convenience in archival storage, the capability of color enhancement, particularly easy transportation by Internet.

Keywords: white-light information processing, tricolor grating, color photography, digital Fourier transform decoding.

1 Developmental history

Optical information processing can be traced back to the beginning of this century when Abbe-Potter first proposed the spatial filtering in a coherent imaging system. They deliberately altered the spatial spectra of the object and obtained different interesting variations in the image[1]. The early success in the optical information processing is the invention of Zernike phase contrast microscopy in the 1930s. By inserting a suitable phase plate and an absorptive plate at the spatial spectrum plane of the coherent system, he directly observed a phase object[2]. Since then the coherent filtering technique has been actively explored to improve the quality of photographs. The most attractive achievement was made by the researchers in the University of Michigan's Radar Laboratory in the 1960s. With a coherent optical system, Cutrona et al. successfully drew a high-resolution terrain map from data collected by a synthetic-aperture radar[3]. Vander Lugt holographically fabricated complex spatial filter and applied it to the coherent system for optical pattern recognition and the signal extraction from additive noise[4]. In the 1970s, coherent optical information processing developed rapidly and was widely used in the fields of optical spectrum analysis, inverse filtering for deconvolution, image differentiation and subtraction, complex filter synthesis, and optical pattern recognition.

However there is inevitable coherent noise in a coherent optical processor, which deteriorates the output image. Furthermore the monochromatic light source limits its applications in multispectrum objects. For these reasons, the group in the Department of Electrical and Electronic Engineering, University of Pennsylvania first carried out the white-light information processing. A typical white-light processor is shown in fig. 1. The this system differs from a coherent processor in having an additional source-encoding mask behind the light source and a diffraction grating at the input plane. The former provides spatial coherence of the system, and the latter provides temporal coherence. Therefore the white-light system performs as perfectly as the coherent system in complex filtering, debluring and image subtraction. Without any coherent noise, the white-light processor possesses the abilities of multi-spectrum processing and wavelength division multiplexing. It has been successfully applied to color image debluring, color image subtraction, pseudocolor encoding, archival storage of color images[5] and restoration of faded color images[6]. White-light information processing enhances the processing capability and opens up new application fields as well. We especially emphasize the pioneering work of refs. [5,6] on the color photography which we will address in this paper.

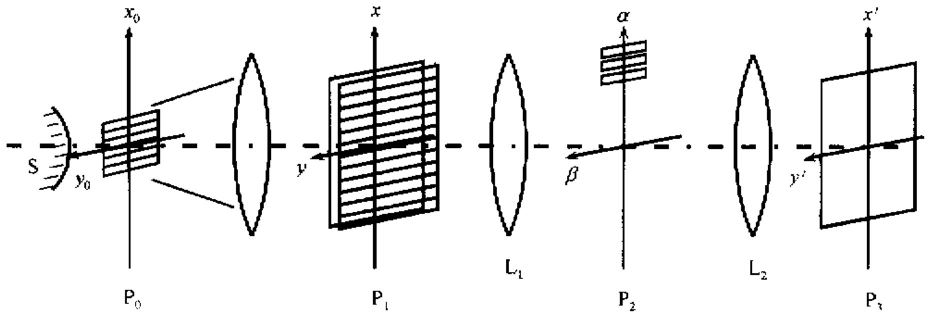

Fig. 1. A typical white-light optical processor. S is the white-light source, P_0 is the source-encoding mask, P_1 is the input plane and diffraction grating, P_2 is the spatial spectrum plane filter, and P_3 is the output plane.

Ref. [5] reported a technique for recording a color image onto a white-and-black film. The film is close-contacted with a Ronchi grating. Three sequential exposures, through red, green, and blue color filters, were done. With each exposure, the Ronchi grating was oriented in a suitable direction. In this way the red, green, and blue primary color information was recorded on the white-and-black film with the grating spatial orientation encoding. For the retrieval of the original color image, the encoded transparency was inserted in the input plane of the white-light processor, and the color filtering at three first-order spectra in the spectrum plane was performed. With the same encoding and decoding principles, ref. [6] reported a technique of color restoration by encoding a color faded image onto white-and-black film and then decoding it with enhanced color filtering in the white-light processor.

Based on the above research, we proposed a technique of one-step color photography with white-and-black films in the 1980s[7]. A specially designed and fabricated tricolor grating was placed at the imaging plane of a normal camera. With this camera, the color information of an object was recorded onto the film at one exposure with grating spatial orientation encoding. It possesses attractive features. As compared with the traditional color photography, it is convenient for archival storage, for the silver halide film has no problem of fading; it is suitable for far-distance photography with poor color saturation, for the decoding is characterized by color enhancement; it is especially suitable for aerial color photography, for the white-and-black film is with large information capacity and low price in cost; it eliminates the environmental pollution, for the organic dye materials are not needed, and only simple chemical materials are used for development. By the middle of the 1980s, the theoretical and experimental study on this technique had been completed, then the researches of instrument and actual applications on this technique had been taken up, yielding two invention patents of China and America[8,9]. There were several key problems to be solved before actual applications. It is a novel engineering project with multi-technology involving optics, mechanics, electronics and computer science[10].

2 Color encoded photography

The color photography with tricolor grating and white-and-black film needs specially fabricated tricolor grating and an encoding camera. The main considerations in the fabrication of the tricolor grating are as follows: (i) color matching, i.e. a stipulating "white" can be composed of red, green and blue of the grating; (ii) the maternal grating used for the fabrication of the tricolor grating should be with suitable space frequency, duty factor and high contrast; (iii) optimum ruling orientations to avoid the overlap of the diffraction orders and the Morie fringes; (iv) high technology in the fabrication to ensure optical level uniformity and flawlessness. The encoding camera is designed so that the tricolor grating is in close contact with the film as a photograph is taken, and they are separated automatically as the film is advancing. We have designed and manufactured three kinds of encoding cameras used for 135, 120 and 180 mm × 180 mm films, respectively. Obviously, it is difficult to fabricate a satisfactory large size tricolor grating. A scheme of color photography with encoding camera is shown in fig. 2.

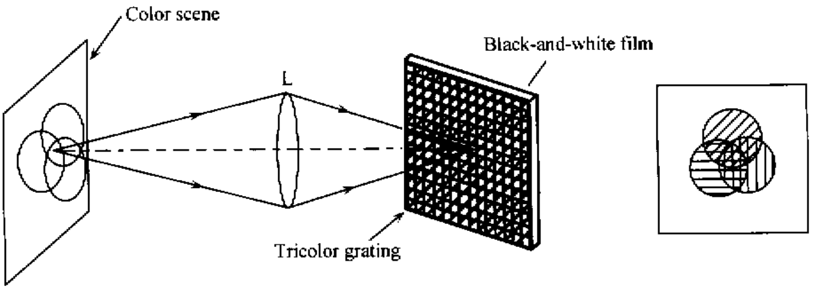

Fig. 2. Color photography with encoding camera.

The intensity distribution at the image plane of the camera can be expressed as

$$T(x, y) = [T_r(x, y)]_R + [T_g(x', y')]_G + [T_b(x'', y'')]_B, \tag{1}$$

where T_r, T_g and T_b are the red, green and blue components of the color image irradiance, respectively, and the green and the blue components have been expressed with the coordinate system of (x', y') and (x'', y''), respectively, for convenience. After exposure and reverse development, the recorded transparency is obtained. When $\gamma = 2$, the corresponding amplitude transmittance is given by[7]

$$T_p(x, y) = T_r(x, y)\left[\frac{1}{2} + \frac{1}{2}\mathrm{sgn}(\cos p_0 x)\right] + T_g(x', y')\left[\frac{1}{2} + \frac{1}{2}\mathrm{sgn}(\cos p_0 x')\right] + T_b(x'', y'')\left[\frac{1}{2} + \frac{1}{2}\mathrm{sgn}(\cos p_0 x'')\right], \tag{2}$$

where p_0 is the spatial frequency of the grating, sgn() is a symbol function. For color image retrieval, the encoded transparency is either inserted into a white-light processor (optical method) or fed into a computer (digital method).

3 Decoding with optical method

The retrieval of color image with optical technique has the advantage of fast operation and two-dimensional parallel processing. However, it needs a special color image decoder. Fig. 3 shows such an optical system designed and manufactured for practical encoded transparency. WS is the indium arc source. LS1 is the achromatic converging system with large numerical aperture, focus $f' = 41.37$ mm and relative apertue $D/f' = 1:0.667$. PIN is the pinhole filter through which a natural spot of the indium arc is formed. LS2 is the achromatic collimating system with the focus $f' = 393.64$ mm, the relative aperture $D/f' = 1:3.5$ and the resolving power in center is 300 lines/mm. P1 is the input plane. LS3 is the specially designed white-light Fourier transform system characterized by achromatic system, with the focus $f' = 376.76$ mm, the relative sperture $D/f' = 1:3.35$, the angle of view $2\omega = 18°$, and the resolving power in center 325 lines/mm. P_2 is the spatial frequency plane. LS4 is a photographic objective, with the focus $f' = 251.19$ mm, the relative sperture $D/f' = 1:9.5$, the area of view $4.8 \text{ mm} \times 6.4$ mm, the angle of view $2\omega = 15°$, and the resolving power in center 120 lines/min. P3 is the CCD image plane. While the encoded transparency of eq. (2) is inserted at P_1, its Fourier spectra can be obtained at P_2, which are composite chromatic with numerous orders. For a specific wavelength λ, the complex light distribution at P_2 can be expressed as

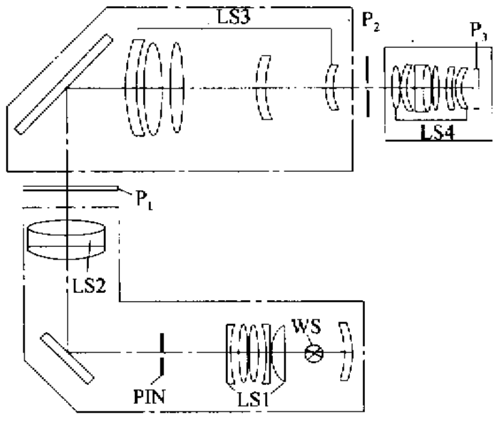

Fig. 3. White-light color image decoder.

$$E(p, q; \lambda) = \int T_p(x, y) \exp[-i(xp + yq)] \mathrm{d}x \mathrm{d}y = T_r(p, q) + \frac{1}{2} \sum_{n=1}^{\infty} a_n T_r(p \pm np_0, q)$$
$$+ T_g(p', q') + \frac{1}{2} \sum_{n=1}^{\infty} a_n T_g(p' \pm np_0, q')$$
$$+ T_b(p'', q'') + \frac{1}{2} \sum_{n=1}^{\infty} a_n T_b(p'' \pm np_0, q''), \quad (3)$$

where (p, q), (p', q') and (p'', q'') are the angular spatial frequency coordinates, and $T_r(p, q)$, $T_g(p', q')$ and $T_b(p'', q'')$ are the Fourier spectra of $T_r(x, y)$, $T_g(x', y')$ and $T_b(x'', y'')$, respectively. The Fourier diffraction orders of the red, green and blue components are spatially separated except for the zero orders. Let three first-order spectra pass the red, green and blue color filter. Then the intensity distribution of the output image can be written as

$$I(x, y) = [T_r^2(x, y)]_R + [T_g^2(x', y')]_G + [T_b^2(x'', y'')]_B, \quad (4)$$

which is the retrieval of the original color image.

4 Digital decoding

The white-light color image decoder specially designed and manufactured is a rather complicated optical system. The requirements of color temperature, aberration, chromatic aberration, field uniformity and elimination of stray light are strict. Besides, they are inflexible in filtering and image processing. In contrast, the digital decoding has the advantages of flexibility and precision and is easy to be set up with commercially available devices. And with the development of computer technology, the operation speed is getting faster and faster. Particularly, it is able to transport the color picture in network in any size.

4.1 Window Fourier transform with integral algorithm

For digital decoding, the encoded transparency is fed into a computer with a scanner. Theoretically, a computer can complete Fourier transform, color filtering, inverse Fourier transform and image synthesis. However, the computing duty of the Fourier transform is so heavy that it takes three hours to decode a 180 mm × 180 mm photograph with a Pentium Ⅱ/233 computer. Therefore a fast decoding algorithm, the window Fourier transform with integral algorithm, was explored.

The encoded transparency is digitized into a discrete image based on the sampling theory. After gamma correction, its amplitude transmittance, with the red, green and blue primary colors denoted by 1, 2 and 3 respectively, is given by[11]

$$f(k, l) = \sum_{m=1}^{3}[T_m(k_m, l_m)]_{\lambda_m}\left[\frac{1}{2} + \frac{1}{2}\operatorname{sgn}(\cos p_0 k_m)\right]_{\lambda_m}, \tag{5}$$

where $k = 0, 1, \cdots, K-1$; $l = 0, 1, \cdots, L-1$; m represents the red, green and blue respectively. Now take a window Fourier transform with a smaller transform window, for instance, a square area of $P \times P$. The Fourier spectra at the first order are given by

$$F(u_m, v_m) = \frac{1}{P^2}\sum_{k=0}^{P-1}\sum_{l=0}^{P-1} f(k, l)\mathrm{e}^{-\mathrm{i}\left(\frac{2\pi}{P}\right)u_m k}\mathrm{e}^{-\mathrm{i}\left(\frac{2\pi}{P}\right)v_m l}, \tag{6}$$

$$u_m = \frac{p_0 P\sin(\theta_m)}{4\pi s}, \quad v_m = \frac{p_0 P\cos(\theta_m)}{4\pi s}, \quad \theta_m = \frac{\pi m}{3},$$

where s is the sampling frequency of the numeralization, θ_m is the angle formed by the grating and x axis. Theoretically, if the transform window includes integral periods of grating, the $F(u_m, v_m)$ represents the average amplitude of the transform windows, corresponding to the modulation frequency of the grating. When the transform window is displaced and overlaid over the whole space of the encoded transparency, the retrieval color image can be obtained.

Obviously, the retrieval color image equals the original image that is smoothed with the transform window. The transform window must be limited to ensure good quality of retrieval color image. If P takes a value of $4\pi s/p_0$, the constructed color image achieves its highest quality which can be represented as

$$I(u, v) = \sum_{m=1}^{3}|F(u_m, v_m)|^2 = \sum_{m=1}^{3}|T_m(x_m, y_m)|^2_{\lambda_m}. \tag{7}$$

With the window Fourier algorithm, not only the large-size Fourier transform is avoided but also the inverse Fourier transform is no longer needed. Therefore the time is shortened considerably. The window Fourier algorithm makes it possible to adopt integer operation for the decoding. This is because (ⅰ) the atomic algorithm needs no sequential inverse Fourier transform, so the precision of the Fourier transform is relaxed; (ⅱ) there is no huge data generated in the local Fourier transform, so the dynamic range of the variables is reduced. Table 1 lists the time-consuming of the digital decoding with different algorithms. With the integral atomic algorithm it only takes three minutes to decode a transparency of 180 mm × 180 mm, which is about 1/60 that with general Fourier transform algorithm.

Table 1 Time-consuming of the digital decoding with different algorithms (unit: second)

Image size (pixel)	Algorithms		
	general FFT of whole block	window Fourier algorithm	integral window Fourier algorithm
1024 × 1024	20	3.5	0.6
2048 × 2048	153	13	2
3500 × 2500(135 film)	332	27	5
18000 × 18000 (aerial film)	11242	1040	179
CPU: Pentium Ⅱ/233MHz, Memory: 64M			

4.2 Fusion of zero-order spectrum in decoding

Theoretically, the retrieval of the color image can be completed by three first-order spectra filtering only on the spatial frequency plane. However, the energy in the first-order diffraction is only 2% that in the zero-order. Additionally, imperfect exposure and development will reduce the signal-to-noise ratio further in the retrieval, and sometimes it can result in local distortion of the retrieval color image. This difficulty can be overcome by fusing zero-order spectrum in the decoding.

Image fusion techniques for enhancing color imagery with low signal-to-noise ratio by fusing the black-and-white imagery with high signal-to-noise ratio to fully utilize complementary information and those for enhancing visual interpretation are becoming an increasingly important component of digital image processing after the 1980s. Several fusing methods, intensity modulation (IM), intensity-hue-saturation (IHS) transformations, high-pass filter (HPF) procedures and multiresolution wavelet decomposition (MWD), have been proposed and used to deal with practical problems[12,13]. The principle of image fusion is based on the fact that the human visual is more sensitive to the spatial details of black and white information than those of other colors. Substituting the intensity of the color image by the black-and-white image with higher signal-to-noise ratio will not distort the color information apperceived by human while enhancing the spatial details.

By IHS transformation method, we merge the image decoded from zero order into the image decoded from first orders to get the final color image. Intensity, hue, and saturation are parameters of human color perception. "Intensity" refers to the total brightness of a color. "Hue" generally refers to the dominant or average wavelength of light contributing to a color. "Saturation" specifies the purity of a color relative to gray. Fundamentally, IHS transformation separates the spatial information as an intensity component from the spectral information in the hue and saturation components of a three-color composite image, thus manipulating independently the spatial information while maintaining the overall color balance of the original scene.

The distortion of decoded image is mainly caused by the lower signal-to-noise ratio of the first orders. Eq. (3) shows that zero-order diffraction is the sum of the diffraction of red, green and blue channels, presenting the brightness of the object. The signal-to-noise ratio of the zero-order diffraction is usually tens of times that of the first-order diffraction in practice. So utilizing the color information of first orders and intensity information of the zero order can efficiently enhance the signal-to-noise ratio of the retrieval image. The IHS fusion transforms the RGB multispectral channels decoded from the first orders into IHS components. To create the merger, the resulting intensity component is replaced by the higher spatial resolution panchromatic data decoded from zero order with small transform window. The transformation is reversed, giving an RGB image with merged panchromatic information. RGB-to-IHS algorithm can be founded in ref. [14]. Beyond their computation speeds, these algorithms differ mainly in the methods used for calculating the intensity component of the transformation. The algorithm of Smith is used and the results are shown in Plate Ⅰ-1, 2, 3. The picture shows that the restore image by using the fusing zero order has a better quality.

5 Color correction

The spectrum character of tricolor grating is the key factor for the color of retrieval image that determines the correctness of retrieval color image. The tricolor grating is designed and fabricated according to the principle of chromatics. In optical decoding method, the three primary colors of the filters accord with that of the tricolor grating, so the original image can be restored correctly.

In the digital decoding method, the retrieval color image is stored as RGB data and displayed on a color monitor. In order to display the true color of the original scene on the monitor, the original scene must be decomposed in to tristimulus values

$$\begin{cases} R(x,y) = \int_{380}^{780} \varphi(x, y, \lambda)\bar{r}(\lambda)\mathrm{d}\lambda, \\ G(x,y) = \int_{380}^{780} \varphi(x, y, \lambda)\bar{g}(\lambda)\mathrm{d}\lambda, \\ B(x,y) = \int_{380}^{780} \varphi(x, y, \lambda)\bar{b}(\lambda)\mathrm{d}\lambda, \end{cases} \tag{8}$$

where $\varphi(x, y, \lambda)$ is the distribution of spectrum energy of scene, and $\bar{r}(\lambda)$, $\bar{g}(\lambda)$ and $\bar{b}(\lambda)$ are the color matching functions of the model of RGB in color television.

The tristimulus values of the retrieval color image can be simulated as

$$T_m(x, y) = \int_{380}^{780} \varphi(x, y, \lambda) C_m(\lambda)\mathrm{d}\lambda, \tag{9}$$

where m represents R, G, and B, and $C_m(\lambda)$ is total spectrum sensitivity that relates to the spectrum character of tricolor grating, the spectrum sensitivity of film and the exposure.

Comparing eq. (8) with eq. (9), if the $C_m(\lambda)$ is equal to the color matching functions $\bar{r}(\lambda)$, $\bar{g}(\lambda)$ and $\bar{b}(\lambda)$, the tristimulus values of the retrieval image correctly represent the color of human perception. Unfortunately, this condition is difficult to be controlled in experiment because of the complexity of film. To solve this problem, we take linear operation of $C_m(\lambda)$ to match the $\bar{r}(\lambda)$, $\bar{g}(\lambda)$ and $\bar{b}(\lambda)$

$$\begin{cases} \bar{r}(\lambda) = m_{11} C_{\mathrm{r}}(\lambda) + m_{12} C_{\mathrm{g}}(\lambda) + m_{13} C_{\mathrm{b}}(\lambda), \\ \bar{g}(\lambda) = m_{21} C_{\mathrm{r}}(\lambda) + m_{22} C_{\mathrm{g}}(\lambda) + m_{23} C_{\mathrm{b}}(\lambda), \\ \bar{b}(\lambda) = m_{31} C_{\mathrm{r}}(\lambda) + m_{32} C_{\mathrm{g}}(\lambda) + m_{33} C_{\mathrm{b}}(\lambda), \end{cases} \tag{10}$$

where m_{ij} is a constant. Multiplying (10) with $\varphi(x, y, \lambda)$ and completing the integration, we have

$$\begin{bmatrix} R(x,y) \\ G(x,y) \\ B(x,y) \end{bmatrix} = \begin{bmatrix} m_{11} & m_{12} & m_{13} \\ m_{21} & m_{22} & m_{23} \\ m_{21} & m_{32} & m_{33} \end{bmatrix} \begin{bmatrix} T_{\mathrm{r}}(x,y) \\ T_{\mathrm{g}}(x,y) \\ T_{\mathrm{b}}(x,y) \end{bmatrix}. \tag{11}$$

The elements of the transform matrix in (11) can be determined by selecting several colors and making the chromatism least. We selected 7 key colors, and obtained the tristimulus values of the retrieval colors through experiments and that of the original colors in the model of RGB in color television. the RGB color space is transfmred to $L^* u^* v^*$ color space for equal perception chromatism, and the chromatism ΔE^*_{uv} is calculated by

$$\Delta E^*_{uv} = [(\Delta L^*)^2 + (\Delta u^*)^2 + (\Delta v^*)^2]^{1/2}. \tag{12}$$

So the total chromatic aberration of the restored system can be expressed as

$$\Delta E_S = \left[\sum_{i=1}^{7} \Delta E_i^2 \right]^{1/2}. \tag{13}$$

Identity matrix is selected as the initial matrix. Using damping least square algorithm and making estimated function equation (13) minimum, we obtain the color correction matrix as follows:

$$\begin{bmatrix} m_{11} & m_{12} & m_{13} \\ m_{21} & m_{22} & m_{23} \\ m_{31} & m_{32} & m_{33} \end{bmatrix} = \begin{bmatrix} 1.042\,9 & -0.244\,5 & -0.084\,0 \\ -0.164\,2 & 1.058\,0 & -0.318\,6 \\ -0.023 & -0.054\,5 & 1.021\,3 \end{bmatrix}. \tag{14}$$

Plate Ⅰ-3 shows the result of retrieval image by using the correctional matrix. The experiment shows that it is viable to use the correctional matrix to correct the retrieval color image and to obtain a good result.

6 Application example in aerial reconnaissance photography

Plate Ⅱ-1 shows a white-and-black encoded transparency acquired with the encoding camera equipped with a 20 lines/mm tricolor grating. The transparency is inserted in the white-light processor of fig. 3, or is fed into a computer for digital processing mentioned in this paper, and the retrieval image is shown in Plate Ⅱ-2, which is quite satisfactory. It can be seen that the color saturation, which is rather low in normal far-distance color photography, is enhanced, showing one of the features of this technique.

At present stage, the color photography with white-and-black films has been applied to some fields, and satisfactory results have been obtained. This equipment, owing to its huge information capacity, large size film, and archival storage, can meet the requirements of aerial photography as well as far-distance ground color photography, because the low color saturation can be enhanced, and the color details of the object can be distinguished.

This technique, which is in steady progress, will find more and more applications, including color restoration of faded color pictures and multispectrum photography[15].

References

1. Porter, A. B., On the diffraction theory of microscope vision, Phil. Mag., 1906, 11(6):154.
2. Zernike, F., Das Phasenkontrastverfahren bei der Mikroskopischen Beobachtung, Z. Tech. Phys., 1935, 16:454.
3. Cutrona, L. J., On the application of coherent optical processing techniques to systhetic aperture radar, Proc. IEEE, 1965, 54:1026.
4. Vander Lugt, A. B., Signal detection by complex spatial filtering, IEEE Trans. Inform. Theory, 1964, IT-10:2.
5. Yu, F. T. S., White-light processing technique for archival storage of color films, Appl. Opt., 1980, 19:2457.
6. Yu, F. T. S., Mu, G. G., Zhuang S. L., Color restoration of faded color films, Opitk, 1981, 58:389.
7. Mu, G. G., Wang, J. Q., Fang, Z. L. et al., A white-light processing technique for color photography with a black-and-white film and a tricolor grating, Chin. J. Sci. Instrum., 1983, 4:124.
8. Mu, G. G., Fang, Z. L., Wang, J. Q. et al., Color photography with black-and-white film, China Patent, CN1003811B, E28, 1989.

9. Mu, G. G., Fang, Z. L., Liu, F. L. et al., Color data image encoding method and apparatus with spectral zonal filter, U. S. Patent, 5452002, 9/1995.
10. Mu, G. G., Fang, Z. L., Liu, F. L. et al., A physical method for color photography, in Trends in Optics, International Commission for Optics, Vol. Ⅲ (ed. Consortini, A.), New York: Academic Press, 1996, 527—542.
11. Jiang, J., Lin, L., Fang, Z. L. et al., Color retrieval of encoded black-and-white film by local fourier transformation algorithm, J. Optoelectronics Laser, 1998, 9(3): 251.
12. Chavez, P. S., Sides, S. C., Anderson, J. A., Comparison of three deferent methods to merge multiresolution and multispectral data: Landsat TM and SPOT panchromatic, Photogrammetric Eng. Remote Sensing, 1991, 57(3): 295.
13. Yocky, A., Image merging and data fusion by means of the discrete two-dimensional wavelet transform, J. Opt. Soc. Am. A, 1995, 12(9): 1834.
14. Smith, A. R., Color gamut transform pairs, Computer Graphics, 1978, 12(3): 12.
15. Mu, G. G., Lin, L., Wang, Z. Q., Multichannel photography with digital Fourier optics, International Trends in Optics and Photonics, ICO Ⅳ (ed. Asakura, T.), Berlin: Springer-Verlag, 1999, 86—95.

LUO Gang et al: Optical/digital color photography based on white-light information processing Plate Ⅰ

1, Encoded white and black; 2, decoded image from first-order spectra; 3, decoded fusing zero-order spectrum.

1, The encoded white-and-black aviation image (original size is 1800 mm × 180 mm); 2, decoded color image.